High supply, high demand: A unique nutrient addition decouples nitrate uptake and metabolism in a large river

by

Michelle Catherine Kelly

Submitted to the graduate degree program in Department of Ecology and Evolutionary Biology and the Graduate Faculty of the University of Kansas in partial fulfillment of the requirements for the degree of Master of Arts.

_____

Dr. Amy J. Burgin, Chairperson

_____

Dr. Admin Husic

_____

Dr. Benjamin A. Sikes

Date Defended: 26 April 2019

The thesis committee for Michelle Catherine Kelly certifies that this
is the approved version of the following thesis:

**High supply, high demand: A unique nutrient addition decouples nitrate uptake and
metabolism in a large river**

_____

Dr. Amy J. Burgin, Chairperson

Date Approved: 26 April 2019

Abstract

Our current understanding of the relationship between nitrate (NO_3^-) uptake and energy cycling in rivers is primarily built on studies conducted in low-nutrient ($NO_3^- < 1$ mg-N L^{-1}), small (discharge < 1 m^3 s^{-1}) systems. Recent advances in sensor technology have allowed for continuous measures of whole-river NO_3^- uptake, allowing us to address how the relationship between nutrient uptake and metabolism changes over time and space during a nutrient addition in a large river. We treated a six-month controlled nitrogen (N) waste release into the Kansas River (conducted by the City of Lawrence, KS) as an ecosystem-scale nutrient addition experiment. We deployed four NO_3^- and dissolved oxygen sensor arrays along a 33 km study reach from February to May 2018 to continuously monitor diel NO_3^--N and stream metabolism. We then evaluated NO_3^- uptake using the extrapolated diel method and modeled stream metabolism using the single station method. We found the highest uptake rates closest to the nutrient release point (866 g-N m^{-2} d^1), despite high NO_3^- supply (4.36 mg-N L^{-1}). Net ecosystem productivity was increasingly autotrophic with distance from the release, with the highest respiration rates observed closest to the release point (7.09 g-O_2 m^{-2} d^1). However, uptake was decoupled from metabolism metrics, likely due to fine-scale hydrologic and biotic factors. Overall, our work sheds light on the ability of large rivers to retain and transform nutrients, while demonstrating that the fine-scale mechanisms that regulate nutrient retention in large rivers are still largely unknown.

Acknowledgements

Table of Contents

Introduction

Nitrogen (N) is a fundamental nutrient, essential to life on Earth (Robertson & Vitousek, 2009). The atmosphere is 78% nitrogen, but in a form (N_2) that is biologically unavailable to most organisms (Erisman et al., 2008). N-fixing bacteria, present in soils and water, transform unreactive N_2 to bio-available ammonia (NH_3), which can be assimilated into plant and microbial biomass. Historically, agriculture was dependent on the activity of N-fixing bacteria, or the application of ammonia-rich manure to replenish soil N. In 1913, Fritz Haber and Carl Bosch developed a cost-effective process that used high temperature, high pressure, and an iron catalyst to synthetically fix ammonia from H_2 and N_2 (Modak, 2002). Over time, the Haber-Bosch process became instrumental in the creation of ammonia products ranging from explosives to fertilizers. Crucially, food production was no longer constrained by bacterial activity and manure supplements. As of 2008, the agricultural boom driven by Haber-Bosch derived N fertilizers was responsible for 48% of world population growth since 1908 (Erisman et al., 2008).

Despite these gains in world population, the development of synthetic N fixation was not without drawbacks. In 2005, 100 Tg of synthetic N was used in global agriculture; however, a relatively small fraction (17 Tg-N) was consumed by humans in crops, dairy, and meat products (Erisman et al., 2008). N is flushed from the land with precipitation, ending up in waterways. Almost 60% of the total annual N delivered from the Mississippi River to the Gulf of Mexico originates from corn and soybean fields, even though this farmland accounts for just 30% of the Mississippi River watershed area (Alexander et al., 2008). Synthetic N-fixation has increased N supply to aquatic ecosystems by a factor of two (Levin et al., 2009; Meybeck, 1982). The ultimate effect of this increased N supply is increased eutrophication, acidification, and deteriorating water quality (Smith et al., 1999; Vitousek et al., 1997). As ammonia-based

fertilizers are leached from agricultural lands, they enter the waterway as ammonium and nitrate. Ammonium and nitrate can easily be incorporated into plant, algae, or microbial biomass. They are a major component in lake and river eutrophication, when out of control biotic growth is caused by an overabundance of a limiting nutrient (Smith et al., 1999). Additionally, when biota die, the decomposition of their biomass consumes oxygen. In extreme cases, this can lead to hypoxic "dead zones" along coastlines (Rabalais et al., 2002; Scavia et al., 2003).

Despite water quality impairment due to N loading, streams and rivers also act as zones of biogeochemical N removal, thereby reducing the downstream impact of N loading. Some removal processes, such as denitrification, are permanent, while others, such as assimilatory uptake, are temporary, with the potential for re-mineralization of N over time. Approximately 15% of N removal in small streams is due to denitrification, with the remaining portion of N removal occurring through assimilatory pathways (Mulholland et al., 2008). Therefore, understanding assimilatory uptake is crucial to understanding total N removal. Assimilatory uptake is performed by both autotrophic (e.g. macrophytes, algae) and heterotrophic (e.g. bacteria, fungi) organisms, as they take up labile N from the water column and assimilate it into biomass. This temporarily lowers in-stream nutrient concentrations, until biota senesce and N is re-released (Hefting et al., 2005). We can conceptualize the amount of dissolved inorganic N that is transformed into particulate organic N as the areal uptake rate (U) per unit area per time (Payn et al., 2005). As U can be strongly affected by ambient nutrient concentrations, we can additionally use uptake velocity (V_f), a measure of biological demand relative to in-stream concentration, to compare the relative efficiency of nutrient removal (Reisinger et al., 2015; Stream Solute Workshop, 1990; Webster et al., 2003). Greater uptake velocity signifies quicker

nutrient uptake, and more efficient nutrient removal. A comprehensive understanding of in-stream uptake is crucial to successfully mitigating increased N loading.

Recently, there has been a push to unite our understanding of riverine energy cycling (e.g. whole-stream metabolism) with novel methods of estimating N uptake from high-frequency sensor data (Bernhardt et al., 2018; Heffernan & Cohen, 2010). Autotrophic assimilation, performed by photosynthetic organisms, can be reflected in measures of whole-stream metabolism, such as gross primary production (GPP) (Covino et al., 2018; Heffernan & Cohen, 2010; Lupon et al., 2016; Reijo et al., 2018). GPP is an estimate of photosynthetic activity based on the amount of oxygen production within a stream or river over the course of a day (Odum, 1956). As primary producers simultaneously photosynthesize and incorporate labile N into biomass, we would expect U to linearly increase with GPP. Additionally, heterotrophic organisms have a similar capacity to incorporate labile N into biomass, which can be reflected in measures of ecosystem respiration (ER). ER is a modeled measure of oxygen consumed by heterotrophs over the course of a day, where greater oxygen consumption can signify greater heterotrophic activity (Christensen et al., 1990). GPP has been shown to correlate with day-night (diel) fluctuations in NO_3^-, suggesting that primary production controls uptake in many streams (Hall & Tank, 2003; Heffernan & Cohen, 2010; Lupon et al., 2016). However, many of these studies have been conducted under conditions that promote high autotrophic growth (e.g. stable hydrology, summertime) and high relative uptake (e.g. low nutrient concentrations with high biotic demand). We suggest that our current understanding of the relationship between riverine energy and nutrient cycling is biased by the lack of studies conducted in large rivers, which can have high nutrient concentrations, unstable hydrology, and low biotic demand.

In this study, we address this gap in knowledge by asking: how does the relationship between nutrient uptake and metabolism change over time and space during a nutrient addition in a large river. We examine three hypotheses: 1) Nearest the release point, where nutrient supply is abundant, gross primary production will be decoupled from nutrient uptake, due to nutrient saturation conditions. 2) Nearest the release point, uptake velocity (e.g. biotic demand relative to concentration) will be lowest, due to nutrient saturation, as biota experience a diminished capacity for nutrient uptake. 3) After the nutrient addition ends and nutrient supply decreases, nutrient uptake will re-couple with gross primary production, as biota no longer experience nutrient saturation conditions. To evaluate these hypotheses, we measured diel NO_3^- concentrations together with stream metabolism during and immediately after a unique six-month N release event on the 8th order Kansas River.

Methods

Study site description and sensor deployment

In 2010, the City of Lawrence, KS ("the City") acquired the property of a former nitrogen fertilizer plant with the intention of remediating the site (Shaw Environmental Inc. 2006, Bond 2017) (The Farmland Manufacturing Plant, Lawrence, KS; Figure 1). Groundwater and surface water on the property were enriched with high N concentrations (0.15 - 33,310 mg NO_3^--N L^{-1}, 0.06-51,640 mg NH_4-N L^{-1}) and previous remediation strategies were not effective at reducing the volume of contaminated water on site. This left surface water storage ponds nearing capacity and in danger of uncontrolled overflows (Bond, 2017; Shaw Environmental Inc., 2006). In late 2017, the Kansas Department of Health and Environment (KDHE) approved the City's request to release 30 million gallons of contaminated surface water from the facility into the Kansas River over a period of six months (November 2017-April 2018). KDHE set strict guidelines for when and how the release was to occur, including: 1) the release must occur between 1 October 2017 and 1 April 2018, 2) total release volume must not exceed 1.9×10^6 L per day, and 3) discharge may only occur when Kansas River flowrate is above 28.3 m^3 s^{-1} (Tom Stiles, KDHE, personal communication). This effectively created a whole-ecosystem experiment wherein a concentrated source of N was released to the river, at a relatively constant rate, over a six-month period.

The Kansas River is a wide, shallow prairie river, with uniformly distributed sandy sediments. About 80% of the river's total drainage area is captured and controlled by reservoirs, which are released intermittently to maintain navigation on the Missouri River (US Army Corps of Engineers, 1984). The USACE conducted a controlled release from the upstream Perry Lake Reservoir from February 23–March 3, 2018 which caused a temporary increase in discharge and decrease in NO_3^- (Figure 2). Additionally, there were significant releases from Tuttle Creek

reservoir (May 8-14) and Milford Lake reservoir (May 18-June 2). Due to the potentially obscuring influence of these reservoir releases on river biogeochemistry, we have selected the date range for data analysis as February 1-May 1, 2018.

We selected four sampling sites (S0-S3) along a 33 km reach of the lower Kansas River (Figure 1). Sampling site selection was highly constrained by river access, as the majority of land adjacent to the riverbank is privately owned. We were able to obtain permission from two private landowners and one company (Bowersock Dam, Lawrence KS) to install sensors. Site S0 (2.5 km upstream from waste release point) was located at the Bowersock Dam in Lawrence, KS, and was gauged by the United States Geological Survey (USGS, gage number 06891080). Site S1 (0.3 km downstream from release) was located 2 m off of the south bank of the Kansas River, in a mixing zone between the release water and the main channel. Site S2 (5.5 km downstream) was located 2 m off of the north bank of the Kansas River, downstream of a channel braid. The final site at DeSoto, KS (S3, 30.6 km downstream) is a fully equipped gauging station managed by the USGS (gage number 06892350), with a sensor array located in the mid-channel.

High frequency UV nitrate sensors (HACH Nitratax plus sc, Loveland, CO) with an optical path length of 2 mm set to a 15-min sampling interval were installed at S0, S1, and S2. Self-cleaning of the sensor was done with a wiper every 5 minutes. These sensors were cross-calibrated with the USGS nitrate sensor at S3 (HACH Nitratax plus sc, Loveland, CO) prior to deployment. Dissolved oxygen and water temperature was collected using PME miniDOT sensors (Vista, California) at 15-min intervals. These were installed at S1 and S2, but not at S0, as hydraulic mixing at the Dam would cause unrepresentative dissolved oxygen readings. At S3, dissolved oxygen and temperature was measured by USGS (www.usgs.org) at 15-min intervals. Photosynthetically active radiation (PAR) data was obtained from the National Ecological

Observatory Network (NEON, www.neonscience.org) monitoring tower at the University of Kansas Field station, located less than 22 km away from the furthest site.

All data was visually inspected using the streamPULSE data cleaning tool (https://data.streampulse.org) and erroneous readings (due to sediment burial or biofilm growth) were removed. Less than 15% of total data points were excluded, the majority of these being at S1 (9.87% of data excluded). For metabolism modeling and nitrate uptake analysis, which required a complete time series of data points, the streamPULSE R package (Package version 0.0.0.9007, R version 3.4.1, R Project for Statistical Computing, Vienna, Austria) was used to fill gaps via linear interpolation (Vlah & Berdanier, 2019). Values based on interpolated data points were then excluded from visualizations and statistical analysis.

Hydrologic modeling

To parameterize the transport of the nitrate plume through the study reach, we modeled dispersion using the advection-dispersion equation (ADE) under mean flow conditions (Van Genuchten et al., 2013). We assumed: 1) flow was uniform in the longitudinal direction, 2) water velocity and nutrient concentration were constant with depth, 3) lateral dispersion was much greater than longitudinal dispersion, and 4) NO_3^- transport was conservative. We recognize that nitrate transformations are occurring in the Kansas River, but assuming conservative transport in this model allowed us to obtain the most conservative estimate of mixing length distance. The model was evaluated for average conditions under the steady-state assumption, using the equations and parameters described in Appendix A of the supplemental material (Admin Husic, personal communication). Under mean flow conditions, the nutrient plume was fully mixed 24 km downstream of the addition site, but was about 75% mixed by 12.50 km downstream (Appendix A).

River metabolism and nutrient uptake modeling

We calculated gross primary production (GPP, g O_2 m^{-2} d^{-1}) and ecosystem respiration (ER, g O_2 m^{-2} d^{-1}) based on the single-station open water exchange method (Odum 1956). We used the streamMetabolizer R package (version 0.10.8) to estimate daily gas exchange rates using a hierarchical Bayesian model (Appling et al., 2017). This model uses water temperature, PAR, and discharge data to predict diurnal DO concentrations and gas exchange rates (Appling et al., 2018).

Daily nitrate uptake due to assimilation (U, g N m^{-2} d^{-1}) was calculated from two-hour averages of 15-min measurements of NO_3^--N using a modified version of the extrapolated diel calculation method (Heffernan & Cohen, 2010) where Q is discharge (L s^{-1}), w is aerial width (m), L is river reach length (m), $[NO_3^-]_{max(0)}$ is the maximum nitrate during the pre-dawn (02:00-08:00) period $[NO_3^-]_{max}$ (mg-N L^{-1}), and $[NO_3^-]_t$ is the nitrate concentration at time of day t (mg-N L^{-1}). We used a standard length of 100 m for each study reach (King et al. 2014). Additionally, composite two-hour nitrate measurements were averaged from 15-minute sampling data, to obtain a more conservative estimate for *Uptake* as discharge was highly variable.

$$U = \frac{Q}{w \cdot L} \sum_{t=0}^{24} \left([NO_3^-]_{max(t=0)} - [NO_3^-]_t\right) \tag{1}$$

Uptake velocity (Vf, mm min^{-1}) was calculated from daily uptake and daily (pre-dawn to pre-dawn) average nitrate concentration, as follows:

$$V_f = \frac{U}{[NO_3^-]} \tag{2}$$

Where U is daily nitrate uptake due to assimilation (g N m^{-2} d^{-1}, Equation 1), and $[NO_3^-]$ is daily average nitrate concentration (mg-N L^{-1}).

Results

Water temperature ranged from a minimum of 0˚C to a maximum of 30˚C, with mean of 12.5˚C. Discharge was variable over the course of the study (S3 mean = 56.1 m^3 s^{-1}, standard deviation = 17.5 m^3 s^{-1}; Table 1), but was historically low for the region (annual mean from 1917-2018 = 194 m^3 s^{-1}, USGS DeSoto gauge data). From February 26, 2018 onwards, upstream NO_3^- concentration was below sensor detection limits (< 0.1 mg-N L^{-1}, verified by grab sampling). S1, nearest the discharge point, experienced the highest NO_3^- concentrations, averaging 5.52 mg-N L^{-1} during the release, and 2.82 mg-N L^{-1} after the release was halted on April 1, 2018. S3 experienced the second highest loading, with 0.63 mg-N L^{-1} during release and 0.22 mg-N L^{-1} post release. S2 experienced the least loading downstream of the release point (mean = 0.33 mg-N L^{-1} during, 0.23 mg-N L^{-1} post). Dissolved organic carbon (DOC) concentrations were highest but most variable at S1 (mean = 11.2 mg L^{-1}, standard deviation = 12.4), which was on average almost twice as DOC-rich as upstream (S0 mean = 5.88 mg L^{-1}, standard deviation = 0.493).

Ecosystem respiration (ER) was highest nearest the discharge point (7.09 g O_2 m^{-2} d^{-1}) and decreased with distance from release (S2 = 4.13 g O_2 m^{-2} d^{-1}, S3 = 1.81 g O_2 m^{-2} d^{-1}, Kruskal-Wallis ANOVA p < 0.001), while gross primary production (GPP) was not directly correlated with proximity to the release input (Figure 3). Mean GPP was significantly different at each site (S1 = 7.51 g O_2 m^{-2} d^{-1}, S2 = 8.51 g O_2 m^{-2} d^{-1}, S3 = 4.55 g O2 m^{-2} d^{-1}, Kruskal-Wallis ANOVA p < 0.001), but did not have as clear a relationship to proximity from the loading site, although the lowest GPP was observed at the most downstream site (S3). Monthly mean GPP significantly increased through time at all sites (Kruskal-Wallis ANOVA, S1

p = 0.023, S2 p = 0.041, S3 p < 0.001). In contrast, only at S3 did monthly mean ER significantly

increase through time (Kruskal-Wallis ANOVA, p < 0.01).

Nitrate uptake decreased with distance from release, a pattern that was consistent both

during (February-March mean S1= 1034 g-N m^2 d^{-1}, S2 = 195 g-N m^2 d^{-1}, S3 = 181 g-N m^2 d^{-1})

and after the release (April mean S1 = 689 g-N m^2 d^{-1}, S2 = 68.7 g-N m^2 d^{-1}, S3 = 18.6 g-N m^2 d^{-1}

^{1}, Figure 4). Monthly mean uptake was significantly different between sites (Kruskal-Wallis

ANOVA, p < 0.001), with highest uptake occurring nearest the Farmland source and rates

generally decreasing downstream. At S1, monthly mean uptake remained elevated post-release

(February-March vs. April, Kruskal-Wallis ANOVA, p = 0.3). However, at both S2 and S3

uptake was significantly lower after release (April) as compared to during the release (February-

March vs. April, Kruskal-Wallis ANOVA; S2 p < 0.001, S3 p < 0.001). Uptake velocity (V_f) was

significantly different across the study reach, with highest V_f at S2 (238 mm min^{-1}) and lowest at

S3 (166 mm min^{-1}, Kruskal-Wallis ANOVA, p = 0.008). Additionally, monthly mean uptake

velocity did not significantly differ during the release period compared to after (February-March

vs. April; Kruskal-Wallis ANOVA, S1 p = 0.39, S2 p = 0.56) except at S3, where mean uptake

velocity significantly decreased in April (p = 0.005).

Uptake metrics were more closely related to gross primary productivity (GPP) than to

ecosystem respiration (ER), but these relationships were not statistically significant (Figure 5,

Figure 6). U was more strongly correlated to GPP (Spearman correlation, S1 R^2 = 0.09, S2 R^2 =

0.03, S3 R^2 = 0.17) than with ER (S1 R^2 < 0.01, S2 R^2 = 0.06, S3 R^2 = 0.07). However, the

relationship between GPP and U was not statistically significant (S1 p = 0.10, S2 p = 0.33)

except at site S3, where the overall relationship between GPP and U was significant (p < 0.01)

but the relationship during the release period (February – March, p = 0.13) and after the release

(April, p = 0.39) were not. Uptake velocity was not related to GPP (Spearman correlation, S1 p = 0.23, S2 p = 0.82, S3 p = 0.31) or to ER (S1 p = 0.78, S2 p = 0.45, S3 = 0.37).

Discussion

We asked how the relationship between nutrient uptake and metabolism would change over time and space in response to a unique nutrient addition in a large river. We hypothesized that gross primary production would be decoupled from uptake at the release point due to nutrient saturation, and the positive relationship between nutrient uptake and primary productivity would be strengthened after the nutrient addition, as biota were no longer nutrient saturated. Elevated N concentrations from the Farmland input (Figure 2) did lead to greater nutrient uptake near the source (Figure 3), but this was not correlated to increased gross primary production (Figure 4). While gross primary production was similar across sites, ecosystem respiration did increase with proximity to the nutrient addition ($p < 0.001$), and net autotrophy (P/R > 1) increased with distance from the release (Kruskal-Wallis ANOVA, $p < 0.001$; Table 1, Figure 3). Although there was no overall relationship between uptake and metabolism, we did see a moderate strengthening in the relationship between U and GPP after the release was concluded (Figure 5), but this was not statistically significant (S1 $p = 0.17$, S2 $p = 0.19$, S3 $p = 0.39$), likely due to many factors, including warmer water and less variable hydrology. In this discussion, we will contextualize our observations of nitrate uptake and metabolism in regard to the wider literature. Additionally, we will explore possible drivers of the decoupled relationship between uptake and stream energetics in this study.

Nitrate uptake

Our knowledge of total nitrate uptake is still constrained by the lack of studies conducted in larger ($Q > 1$ m^3 s^{-1}) systems; despite a meta-analysis done by Tank et al. (2008) over a decade ago, this remains a problem for the field. We have synthesized meta-analysis data compiled by Tank et al. (2008) to provide context for our results (Figure 7). Generally, nitrate uptake (U) and

uptake velocity (V_f) increase with higher river discharge; however, it is difficult to fully evaluate this relationship when the vast majority of uptake studies are conducted in lower discharge (< 1 $m^3 s^{-1}$) systems. Despite this, our values of uptake fit within the range predicted by the linear regression presented in Tank et al. 2008, although they are the among the highest rates reported in the literature (Figure 7, Panel C). V_f in this study were similarly high in comparison to those summarized by Tank et al. (Figure 7, Panel D), but not outside of the measured range.

High nutrient concentrations promoted high uptake and reduced downstream nitrate concentration, unlike other studies (e.g. Marti et al., 2004). We expected biota to be saturated under high N supply, causing the lowest uptake rates nearest the release point. Instead we found the highest uptake rates nearest the release point. A possible explanation for this result is that we were unable to install equipment and begin sampling until ~3 months after the City began pumping waste from their facility. We may have missed a "priming period" where biota were initially supersaturated, but instead captured what was increased uptake over time after "adapting" to high N supply. Additionally, V_f remained elevated at each site except for the site furthest downstream from the release ($p < 0.01$), suggesting that the release had a lasting impact on the capacity for nutrient uptake at S1 and S2. Therefore, the release pulse did facilitate greater nutrient processing in the Kansas River, but further analysis would be necessary to understand the specific drivers of increased uptake and how long this affect lasted.

Stream metabolism

Understanding large river metabolism has become a focus of the field in recent years, as synthesis work has allowed us to better understand the relationship between stream size and system energetics (Dodds et al., 2013; Hall et al., 2016; Young et al., 2008). The Kansas River is 8th order in our study reach; as such, it adds a valuable large river data point to syntheses of

13

whole river metabolism. We found the Kansas River to be increasingly autotrophic with distance from the nutrient release (P/R S1 = 1.30, S2 = 4.70, S3 = 5.62; Kruskal-Wallis ANOVA, p < 0.001). For context, Dodds et al. measured whole-stream metabolism in the Kansas River (8th order) and found the system to be dominantly heterotrophic (GPP = 8.48 g O_2 m^{-2} d^{-1}, |ER| = 12.12 g O_2 m^{-2} d^{-1}) (2008), but this discrepancy may be due in part to the seasonal or site differences between our two studies (Dodds et al. was conducted 180 km upstream of our sites and during autumn). In comparison to other rivers, GPP was relatively high in this study (Figure 7A), but was well predicted by the general relationship between stream size and metabolism as explored by Hall et al. (2016). In context, this suggests that our system was highly productive, despite cold water temperatures in February (mean = 2.9˚C) and March (mean = 9.2˚C), which likely suppressed primary productivity's response to increased nutrient loading.

Ecosystem respiration was within the low to medium range of values summarized by Hall et al. (2016), but similar to ER measured in other higher order rivers (Figure 6B). ER rates are greatly affected by benthos substrate type, available organic matter, and hyporheic zone connectivity (Young et al., 2008). The Kansas River is a lowland river with a highly homogeneous, sandy substrate; thus, hyporheic zone flow and sediment redox conditions are unlikely to be significantly different between sites. This suggests that the high to low ER gradient observed across sites is not primarily driven by either of these two factors. High dissolved organic carbon (DOC, Table 1) from the release likely drove high decomposition rates, causing ER to peak nearest the release point and decrease downstream. DOC input could also have catalyzed an increase in whole-river denitrification. However, we posit that this was unlikely, as the Kansas River is well oxygenated with coarse grained, sandy sediment, which generally does not promote the redox conditions necessary for high denitrification activity.

(De)coupled metabolism and nitrate dynamics

We found no significant relationship between nutrient uptake and GPP, regardless of distance from the nutrient release (Figure 5). Multiple studies have shown a positive relationship between nitrate uptake and GPP (Covino et al., 2018; Heffernan & Cohen, 2010; Lupon et al., 2016), but these studies have been conducted under relatively low (< 1 mg NO_3-N L^{-1}) nutrient conditions. To our knowledge, only one other study has investigated the relationship between nitrate uptake and primary productivity in an N-rich (mean 3.66 mg NO_3-N L^{-1}) river, finding a positive relationship between the two parameters only when discharge was low (< 0.45 m^3 s^{-1}, Rode et al. 2016).

In our study, metabolic rates were much more closely related to water temperature than nutrient uptake, likely due to the winter-spring transition period. During April, when water temperatures were warmer (mean = 12˚C) the relationship between GPP and U became stronger but was not statistically significant (February-March, $R^2 < 0.01$, $p = 0.43$; April, $R^2 = 0.03$, $p = 0.31$). Additionally, hydrology was considerably more stable during April (SD = 2.3 m^3 s^{-1}), than during February and March (SD = 17 m^3 s^{-1}), which likely obscured the relationship. As opposed to findings by Rode et al. (2016), where near-baseflow low discharge was a critical factor in observing tightly coupled GPP and uptake, we suggest that discharge variability is a more important factor, and that these coupled relationships can likely be evident in higher order systems at high flow, as long as discharge is not highly variable.

An additional explanation for the decoupled relationship between uptake and metabolism is that the pulse addition itself may have enhanced biogeochemical transformation rates. Nitrification (NH_3 or $NH_4^+ \rightarrow NO_3^-$) may distort the diel nitrate signal (Harrison et al., 2005), driving an increase in nitrate as biota are simultaneously removing it through uptake pathways.

15

This may confound estimates of U calculated using the extrapolated diel method, as this calculation assumes that all diel change in nitrate concentration is due to uptake processes. As ammonium concentrations at the release point were not different from upstream concentrations (Table 1), it's unlikely that the waste release significantly increased riverine nitrification. Additionally, if the release pulse caused denitrification rates to increase, this could further drive decoupling between GPP and U. If DOM from the release pulse (Table 1) increased decomposition rates, the subsequently elevated ER would be decoupled from estimates of nitrate uptake. As discussed previously, we don't think that whole-river denitrification was a driving mechanism of NO_3^- removal in this study, but even low rates of denitrification have the potential to obscure the relationship between NO_3^- uptake estimates and modeled ER.

Conclusions

In this study, a controlled nitrogen waste release by the City of Lawrence, KS, dramatically increased nutrient availability in the Kansas River. We predicted that nutrient uptake would be saturated in response to an extreme increase in nutrient supply, but this was not the case. High uptake rates were observed along the study reach, with the highest rates occurring where nutrient supply was also highest, regardless of ambient N concentration. This signifies that the study reach had a high capacity for nutrient removal. Unlike general trends observed in the literature, nitrate uptake was not well predicted by gross primary productivity, likely due to hydrologic variability and low water temperatures in February and March. To our knowledge, this is the largest river where nitrate uptake rates have been measured, adding to the growing body of work investigating nutrient retention in large rivers. Overall, our work further highlights the lack of knowledge regarding the mechanisms that regulate nutrient retention in large rivers.

Table 1. Overall mean conditions from February 1, 2018 to May 1, 2018, with standard deviations in brackets. Q = discharge. NH4+ = water column ammonium concentration. NO3 = water column nitrate concentration. DOC = dissolved organic carbon, measured using non-purgeable organic carbon (NPOC) method. GPP = gross primary productivity. |ER| = absolute value of ecosystem respiration. P/R = ratio of gross primary productivity to ecosystem respiration (P/R = GPP/|ER|). U = nitrate uptake. Vf = nitrate uptake velocity. NA = data not collected or data not modeled. * = detection limit for nitrate measurements was 0.1 mg-N L⁻¹. † = Value is an average of biweekly grab sample measurements.

| Site	Sensor placement	Q (m³ s⁻¹)	NH₄ (mg-N L⁻¹)†	NO₃ (mg-N L⁻¹)*	DOC (mg L⁻¹)†	GPP (g O₂ m⁻² d⁻¹)	|ER| (g O₂ m⁻² d⁻¹)	P/R	U (g-N m² day⁻¹)	V_f (mm min⁻¹)
S0	Dam inflow	50.4 (17.5)	0.047 (0.032)	0.118 (0.045)	5.88 (0.493)	NA	NA	NA	NA	NA
S1	South bank	44.9 (14.7)	0.048 (0.024)	4.36 (2.06)	11.2 (12.4)	7.51 (3.02)	7.09 (3.73)	1.30 (0.747)	866 (665)	184 (152)
S2	North bank	50.6 (17.8)	0.058 (0.027)	0.294 (0.197)	5.78 (0.521)	8.51 (3.49)	4.13 (3.48)	4.70 (7.71)	109 (105)	238 (175)
S3	Mid-channel	56.1 (17.5)	0.084 (0.064)	0.490 (0.275)	6.24 (0.844)	4.55 (3.68)	1.81 (2.06)	5.62 (17.9)	144 (186)	165 (177)
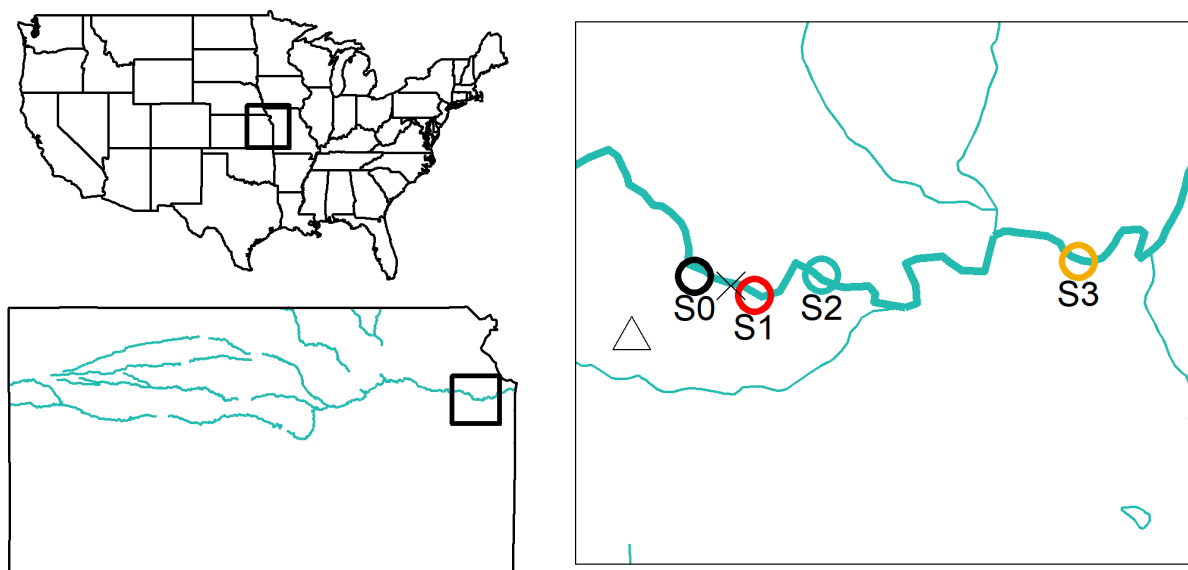
Figures

Figure 1. Map of USA with study area outlined in the black box (top left). Map of the state of Kansas, with major rivers within the Kansas River watershed denoted in light blue, and the study area outlined in the black box (bottom left). The Kansas River study reach, with sensor sites indicated by colored circles and site name labels (S0-S3; right). X = the nutrient release site. Δ = The City of Lawrence. Smaller tributary streams are (from west to east) the Wakarusa River, Stranger Creek, and Kill Creek.
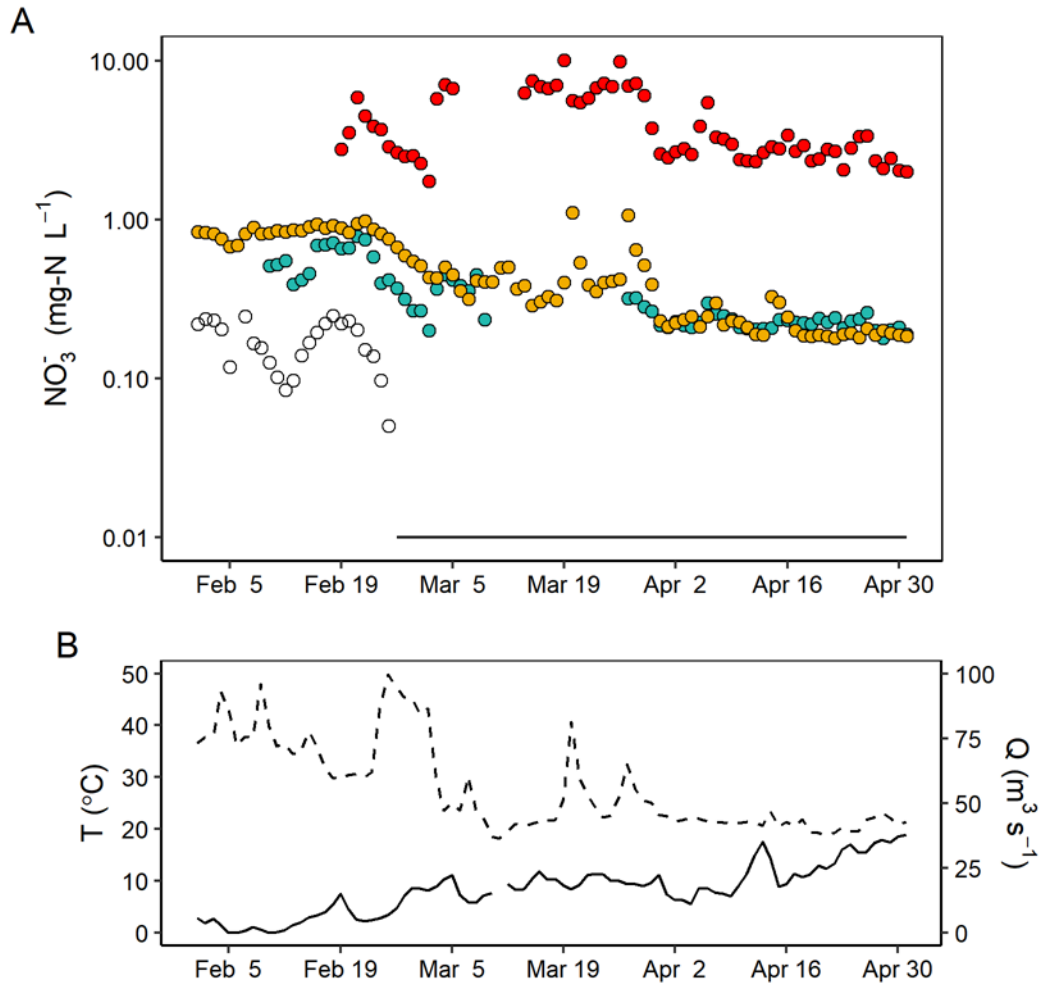
Figure 2. Mean daily nitrate (NO_3^-) concentration at each study site (A). S0 = black, S1 = red, S2 = blue, S3 = yellow. From February 26, 2018 onwards nitrate at S0 was < 0.01 mg-N L^{-1} (black line). Mean daily water temperature (T, solid line) and discharge (Q, dashed line) at S3 (B).
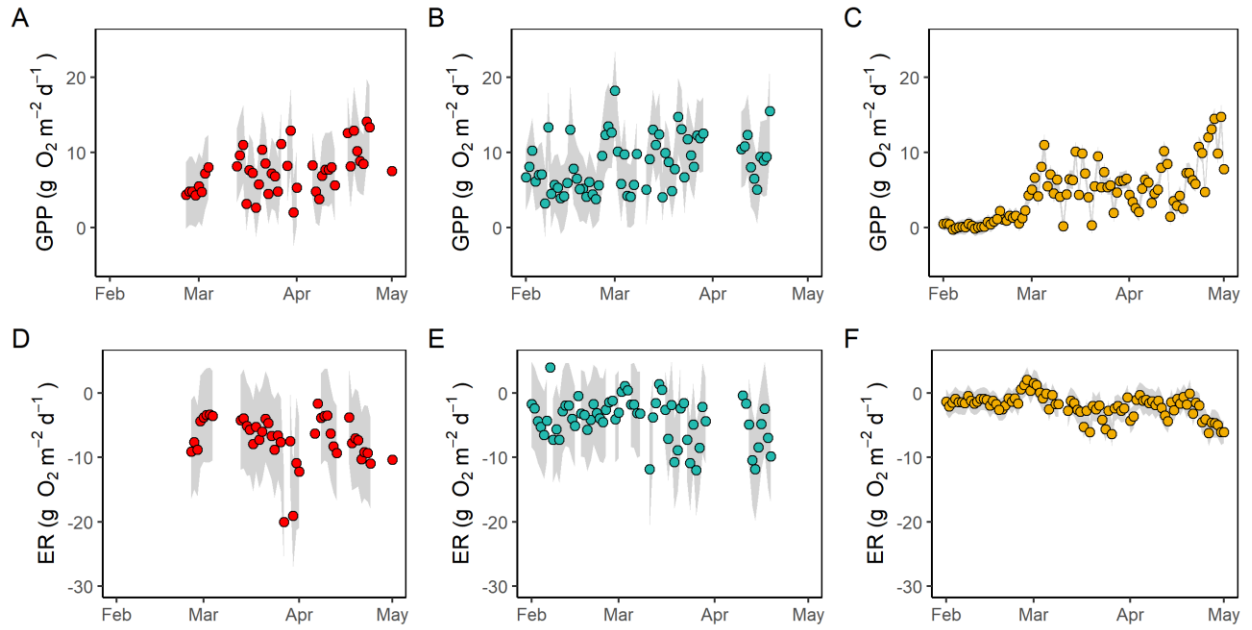
Figure 3. Modeled estimates of gross primary productivity (GPP) at S1 (A), S2 (B), and S3 (C). Ecosystem respiration (ER) at S1 (D), S2 (E) and S3 (F). Grey bars denote 95% confidence interval.
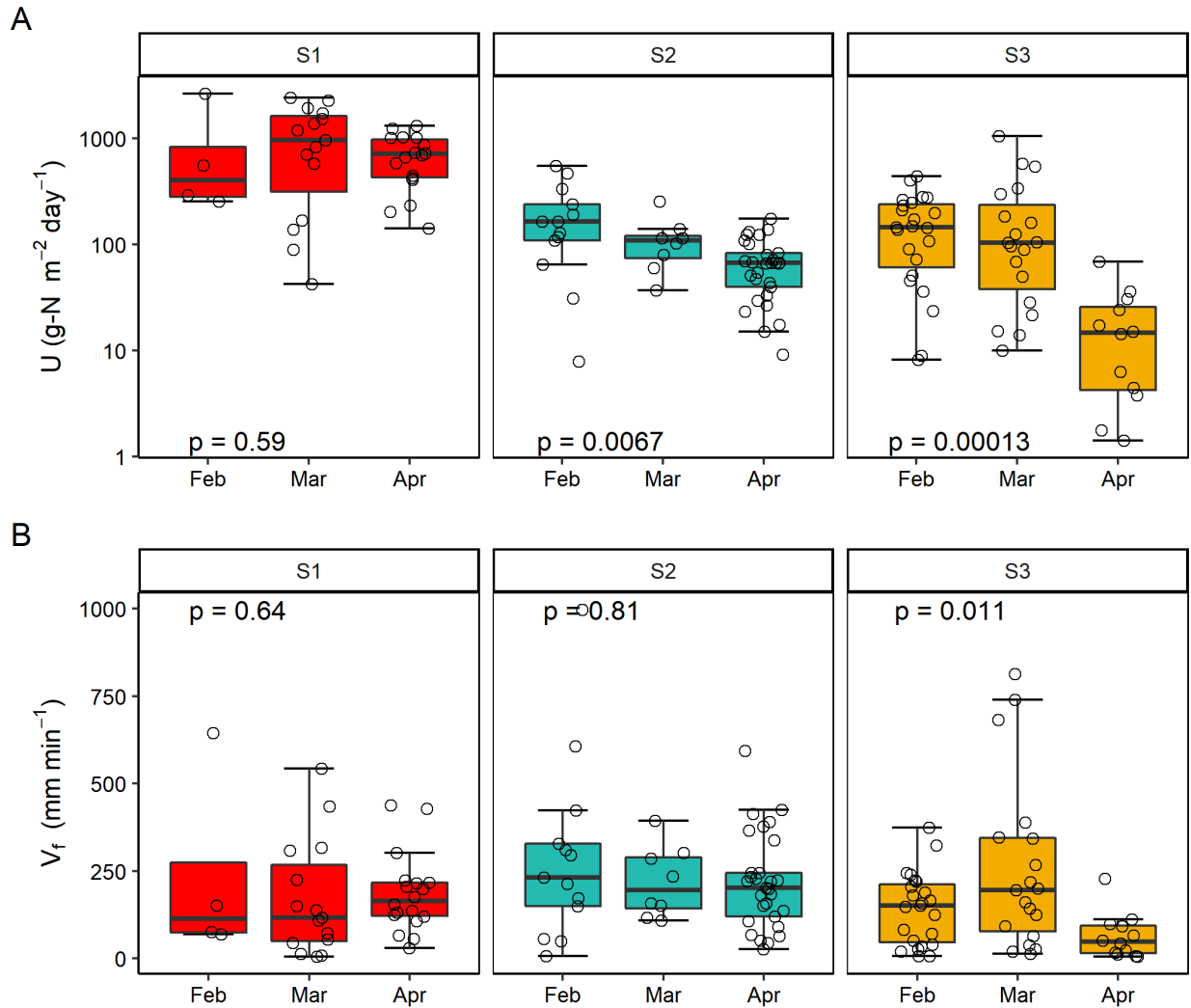
Figure 4. Nitrate uptake due to assimilation (U) for S1, S2, and S3 (A). Nitrate uptake velocity (Vf) for S1, S2, and S3 (B). Open circles denote data for one day. Horizontal bar of box plot denotes median, lower hinge denotes first quartile, upper hinge denotes third quartile, upper whiskers denote the third quartile plus 1.5 times the interquartile range, and lower whiskers denote the first quartile minus 1.5 times the interquartile range.
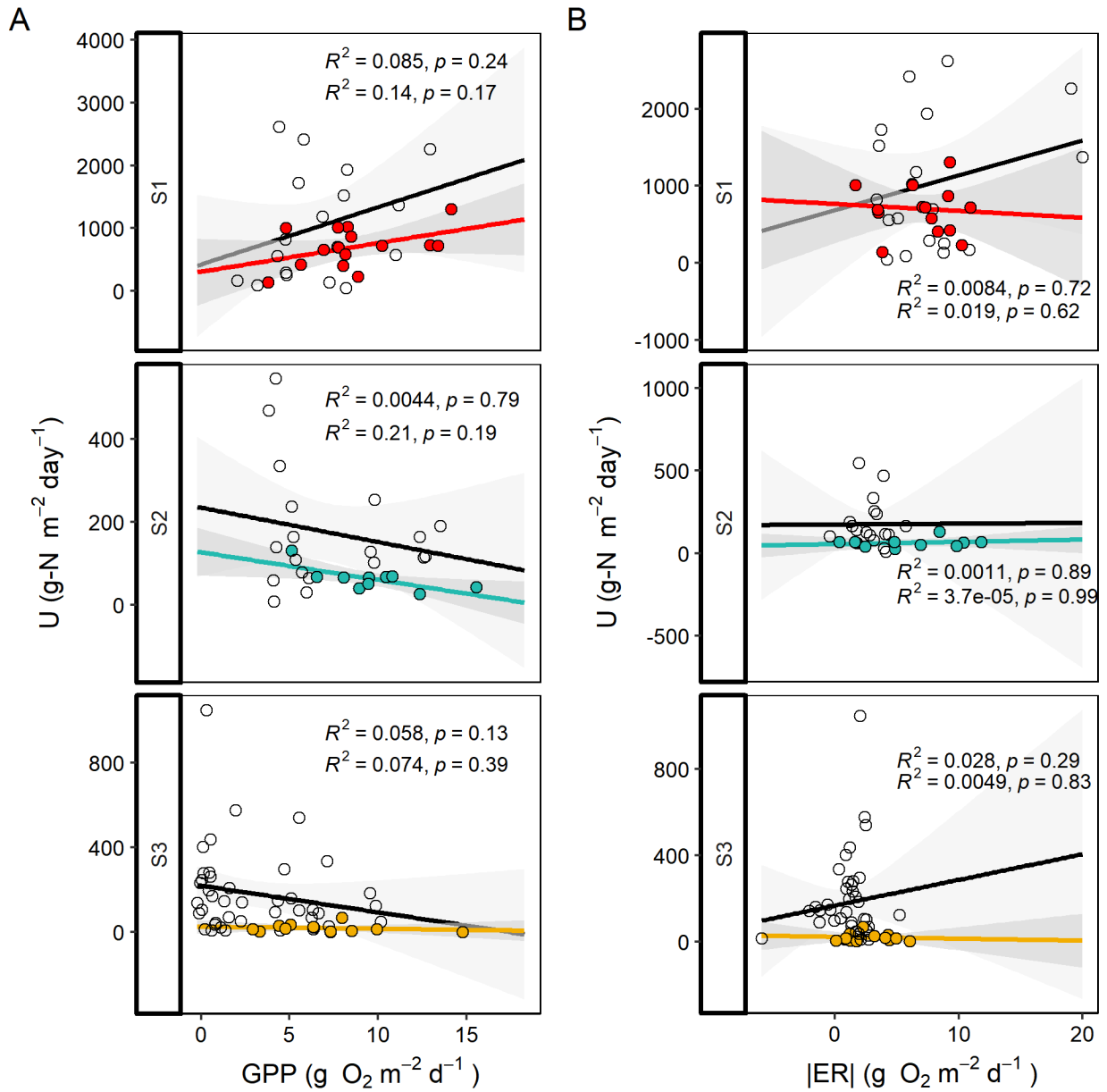
Figure 5. Relationships between gross primary productivity (GPP) and nitrate uptake (U, panel A) and relationships between ecosystem respiration (ER) and nitrate uptake (B). Black and white data points represent February and March, 2018, with corresponding R^2 and p value for linear regression (black line) on top. Colored data points represent April, 2018, with corresponding R2 and p values for linear regression (colored line) beneath.

Figure 6. Relationships between gross primary productivity (GPP) and nitrate uptake velocity (V_f, panel A) and relationships between ecosystem respiration (ER) and nitrate uptake velocity (B). Black and white data points represent February and March, 2018, with corresponding R^2 and p value for linear regression (black line) on top. Colored data points represent April, 2018, with corresponding R2 and p values for linear regression (colored line) beneath.
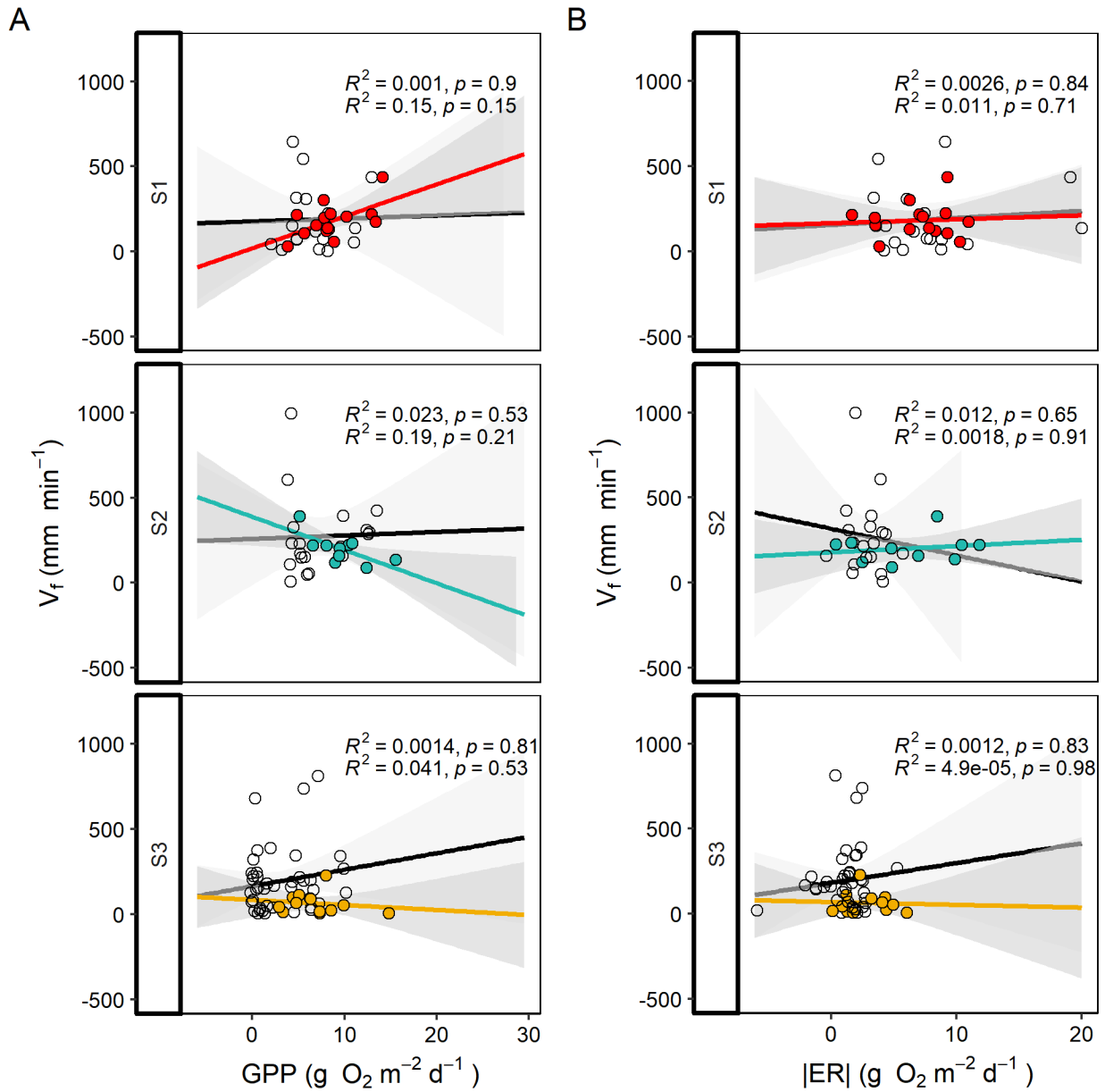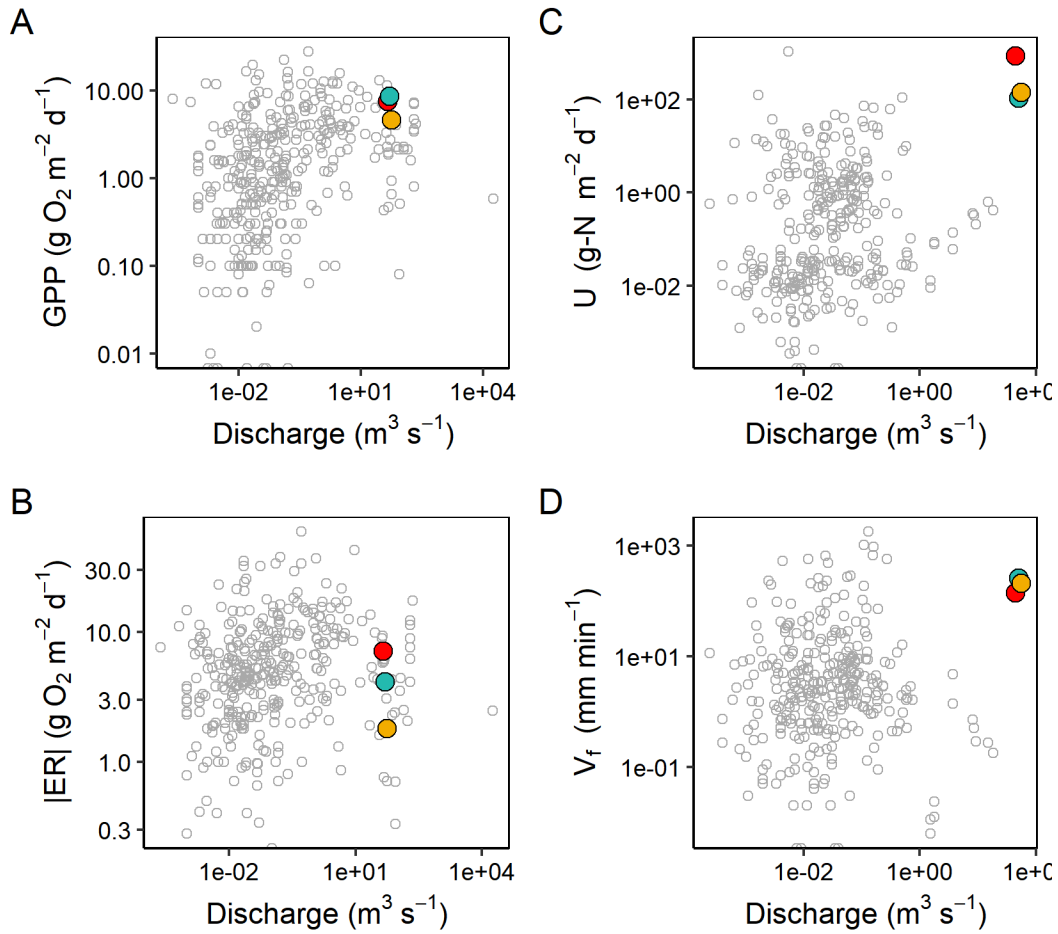
Figure 7. Meta-analysis of previously published results of (A) GPP, (B) ER (where grey points are data summarized by Hall et al. 2016), and (C) U, (D) Vf compared to stream discharge (where grey points are data from Rode et al. 2016, Hensley et al. 2014, and data summarized by Tank et al. 2008, with U calculated as $U = V_f / [NO_3^-]$) plus mean results from this study (where red = S1, blue = S2, yellow = S3).

References

Alexander, R. B., Smith, R. A., Schwarz, G. E., Boyer, E. W., Nolan, J. V., & Brakebill, J. W. (2008). Differences in Phosphorus and Nitrogen Delivery to The Gulf of Mexico from the Mississippi River Basin. *Environmental Science & Technology*, *42*(3), 822–830. https://doi.org/10.1021/es0716103

Appling, A. P., Hall, R. O., Arroita, M., & Yackulic, C. B. (2017). *streamMetabolizer: Models for Estimating Aquatic Photosynthesis and Respiration*. Retrieved from https://github.com/USGS-R/streamMetabolizer

Appling, A. P., Hall, R. O., Yackulic, C. B., & Arroita, M. (2018). Overcoming Equifinality: Leveraging Long Time Series for Stream Metabolism Estimation. *Journal of Geophysical Research: Biogeosciences*, *123*(2), 624–645. https://doi.org/10.1002/2017JG004140

Bernhardt, E. S., Heffernan, J. B., Grimm, N. B., Stanley, E. H., Harvey, J. W., Arroita, M., et al. (2018). The metabolic regimes of flowing waters: Metabolic regimes. *Limnology and Oceanography*, *63*(S1), S99–S118. https://doi.org/10.1002/lno.10726

Bond, M. (2017, June 30). Excess Nitrate Impacted Ground Water. KDHE Pump Shutoff Request.

Christensen, P. B., Nielsen, L. P., Sørensen, J., & Revsbech, N. P. (1990). Denitrification in nitrate-rich streams: Diurnal and seasonal variation related to benthic oxygen metabolism. *Limnology and Oceanography*, *35*(3), 640–651. https://doi.org/10.4319/lo.1990.35.3.0640

Covino, T. P., Bernhardt, E. S., & Heffernan, J. B. (2018). Measuring and interpreting relationships between nutrient supply, demand, and limitation. *Freshwater Science*, *37*(3), 448–455. https://doi.org/10.1086/699202

Dodds, Veach, A. M., Ruffing, C. M., Larson, D. M., Fischer, J. L., & Costigan, K. H. (2013). Abiotic controls and temporal variability of river metabolism: multiyear analyses of Mississippi and Chattahoochee River data. *Freshwater Science*, *32*(4), 1073–1087. https://doi.org/10.1899/13-018.1

Dodds, W. K., Beaulieu, J. J., Eichmiller, J. J., Fischer, J. R., Franssen, N. R., Gudder, D. A., et al. (2008). Nitrogen cycling and metabolism in the thalweg of a prairie river: RIVER NITROGEN CYCLING. *Journal of Geophysical Research: Biogeosciences*, *113*(G4). https://doi.org/10.1029/2008JG000696

Erisman, J. W., Sutton, M. A., Galloway, J., Kilmont, Z., & Winiwarter, W. (2008). How a century of ammonia synthesis changed the world. *Nature Geoscience*, *1*, 636–639. https://doi.org/10.1038/ngeo325

Hall, Tank, J. L., Baker, M. A., Rosi-Marshall, E. J., & Hotchkiss, E. R. (2016). Metabolism, Gas Exchange, and Carbon Spiraling in Rivers. *Ecosystems*, *19*(1), 73–86. https://doi.org/10.1007/s10021-015-9918-1

Hall, R. J. O., & Tank, J. L. (2003). Ecosystem metabolism controls nitrogen uptake in streams in Grand Teton National Park, Wyoming. *Limnology and Oceanography*, *48*(3), 1120–1128. https://doi.org/10.4319/lo.2003.48.3.1120

Harrison, J. A., Matson, P. A., & Fendorf, S. E. (2005). Effects of a diel oxygen cycle on nitrogen transformations and greenhouse gas emissions in a eutrophied subtropical stream. *Aquatic Sciences*, *67*(3), 308–315. https://doi.org/10.1007/s00027-005-0776-3

Heffernan, J. B., & Cohen, M. J. (2010). Direct and indirect coupling of primary production and diel nitrate dynamics in a subtropical spring-fed river. *Limnology and Oceanography*, *55*(2), 677–688. https://doi.org/10.4319/lo.2010.55.2.0677

Hefting, M. M., Clement, J.-C., Bienkowski, P., Dowrick, D., Guenat, C., Butturini, A., et al. (2005). The role of vegetation and litter in the nitrogen dynamics of riparian buffer zones in Europe. *Ecological Engineering*, *24*(5), 465–482. https://doi.org/10.1016/j.ecoleng.2005.01.003

Huai, W., Shi, H., Yang, Z., & Zeng, Y. (2018). Estimating the Transverse Mixing Coefficient in Laboratory Flumes and Natural Rivers. *Water, Air, and Soil Pollution*, *229*(252), 1–17. https://doi.org/10.1007/s11270-018-3893-z

Levin, L. A., Ekau, W., Gooday, A. J., Jorissen, F., Middelburg, J. J., Naqvi, W., et al. (2009). Effects of natural and human-induced hypoxia on coastal benthos. *Biogeosciences Discussions*, *6*, 3563–3654.

Lupon, A., Martí, E., Sabater, F., & Bernal, S. (2016). Green light: gross primary production influences seasonal stream N export by controlling fine-scale N dynamics. *Ecology*, *97*(1), 133–144. https://doi.org/10.1890/14-2296.1

Marti, E., Aumatell, J., Gode, L., Poch, M., & Sabater, F. (2004). Nutrient Retention Efficiency in Streams Receiving Inputs from Wastewater Treatment Plants. *Journal of Environmental Quality*, *33*, 285–293. https://doi.org/10.2134/jeq2004.2850

Meybeck, M. (1982). Carbon, Nitrogen, and Phosphorus Transport By World Rivers. *American Journal of Science*, *282*, 401–450.

Modak, J. M. (2002). Haber process for ammonia synthesis. *Resonance*, *7*(9), 69–77. https://doi.org/10.1007/bf02836187

Mulholland, P. J., Helton, A. M., Poole, G. C., Hall, R. O., Hamilton, S. K., Peterson, B. J., et al. (2008). Stream denitrification across biomes and its response to anthropogenic nitrate loading. *Nature*, *452*(7184), 202–205. https://doi.org/10.1038/nature06686

Odum, H. T. (1956). Primary Production in Flowing Waters. *Limnology and Oceanography*, *1*(2), 102–117. https://doi.org/10.4319/lo.1956.1.2.0102

Payn, R. A., Webster, J. R., Mulholland, P. J., Valett, H. M., & Dodds, W. K. (2005). Estimation of stream nutrient uptake from nutrient addition experiments: Estimation of stream nutrient uptake. *Limnology and Oceanography: Methods*, *3*(3), 174–182. https://doi.org/10.4319/lom.2005.3.174

Rabalais, N. N., Turner, R. E., & Wiseman, W. J. (2002). Gulf of Mexico Hypoxia, A.K.A. "The Dead Zone." *Annual Review of Ecology and Systematics*, *33*(1), 235–263. https://doi.org/10.1146/annurev.ecolsys.33.010802.150513

Reijo, C. J., Hensley, R. T., & Cohen, M. J. (2018). Isolating stream metabolism and nitrate processing at point-scales, and controls on heterogeneity. *Freshwater Science*, *37*(2), 238–250. https://doi.org/10.1086/697319

Reisinger, A. J., Tank, J. L., Rosi-Marshall, E. J., Hall, R. O., & Baker, M. A. (2015). The varying role of water column nutrient uptake along river continua in contrasting landscapes. *Biogeochemistry*, *125*(1), 115–131. https://doi.org/10.1007/s10533-015-0118-z

Robertson, G. P., & Vitousek, P. M. (2009). Nitrogen in Agriculture: Balancing the Cost of an Essential Resource. *Annual Review of Environment and Resources*, *34*(1), 97–125. https://doi.org/10.1146/annurev.environ.032108.105046

Scavia, D., Rabalais, N. N., Turner, R. E., Justić, D., & Wiseman, W. J. (2003). Predicting the response of Gulf of Mexico hypoxia to variations in Mississippi River nitrogen load. *Limnology and Oceanography*, *48*(3), 951–956. https://doi.org/10.4319/lo.2003.48.3.0951

Shaw Environmental Inc. (2006). *Site Characterization Report, Former Farmland Nitrogen Plant, Lawrence, Kansas*.

Simons, Li, & Associates, I. (1984). *Final report for analysis of channel degradation and bank erosion in the lower Kansas River*. Kansas City.

Smith, V. H., Tilman, G. D., & Nekola, J. C. (1999). Eutrophication: impacts of excess nutrient inputs on freshwater, marine, and terrestrial ecosystems. *Environmental Pollution*, *100*(1–3), 179–196. https://doi.org/10.1016/S0269-7491(99)00091-3

Stream Solute Workshop. (1990). Concepts and Methods for Assessing Solute Dynamics in Stream Ecosystems. *Journal of the North American Benthological Society*, *9*(2), 95–119. https://doi.org/10.2307/1467445

Tank, J. L., Rosi-Marshall, E. J., Baker, M. A., & Hall, R. O. (2008). ARE RIVERS JUST BIG STREAMS? A PULSE METHOD TO QUANTIFY NITROGEN DEMAND IN A LARGE RIVER. *Ecology*, *89*(10), 2935–2945. https://doi.org/10.1890/07-1315.1

US Army Corps of Engineers. (1984). *Analysis of Channel Degradation and Bank Erosion in the Lower Kansas River* (MRD Sediment Series No. 35) (p. 318). Kansas City District: US Army Corps of Engineers.

Van Genuchten, M. T., Leij, F. J., Skaggs, T. H., Toride, N., Bradford, S. A., & Pontedeiro, E. M. (2013). Exact analytical solutions for contaminant transport in rivers 1. The equilibrium advection-dispersion equation. *Journal of Hydrology and Hydromechanics*, *61*(2), 146–160. https://doi.org/10.2478/johh-2013-0020

Vitousek, P. M., Aber, J. D., Howarth, R. W., Likens, G. E., Matson, P. A., Schindler, D. W., et al. (1997). Human Alteration of the Global Nitrogen Cycle: Sources and Consequences. *Ecological Applications*, *7*(3), 737–750. https://doi.org/10.1890/1051-0761(1997)007[0737:haotgn]2.0.co;2

Vlah, M., & Berdanier, A. (2019). *StreamPULSE: Run Stream Metabolism Models on StreamPULSE data*. Retrieved from https://github.com/streampulse/StreamPULSE

Webster, J. R., Mulholland, P. J., Tank, J. L., Valett, H. M., Dodds, W. K., Peterson, B. J., et al. (2003). Factors affecting ammonium uptake in streams - an inter-biome perspective. *Freshwater Biology*, *48*(8), 1329–1352. https://doi.org/10.1046/j.1365-2427.2003.01094.x

Young, R. G., Matthaei, C. D., & Townsend, C. R. (2008). Organic matter breakdown and ecosystem metabolism: functional indicators for assessing river ecosystem health. *Journal of the North American Benthological Society*, *27*(3), 605–625. https://doi.org/10.1899/07-121.1

Appendix A: Advective-Dispersion Model

To describe the distance which it takes the Farmland Plant nitrogen input to fully mix across the Kansas River, we modeled the advection-dispersion equation (ADE). The three-dimensional ADE for non-conservative transport in uniform flow can be described as:

$$\frac{\partial C}{\partial t} = -u\frac{\partial C}{\partial x} + D_x\frac{\partial^2 C}{\partial x^2} + D_y\frac{\partial^2 C}{\partial y^2} + D_z\frac{\partial^2 C}{\partial z^2} - kC \tag{1}$$

where C is the concentration of nitrate (mg L^{-1}), t is time (s), x, y, and z are distance in the longitudinal, lateral, and vertical directions, respectively (m), u is velocity in the x direction (m s^{-1}), D_x is the longitudinal dispersion coefficient (m^2 s^{-1}), D_y is the lateral dispersion coefficient (m^2 s^{-1}), D_z is the vertical dispersion coefficient (m^2 s^{-1}), and k is the first-order decay coefficient (s^{-1}).

We made the following assumptions: 1) uniform flow conditions in the longitudinal direction, 2) depth-averaged velocity and concentration profiles (i.e. no changes in the z direction), 3) lateral dispersion was much greater than longitudinal dispersion, and 4) conservative transport of nitrate. Although transformations of nitrate do occur within the Kansas River, we assume that these transformations do not significantly affect the mixing length distance. Given these assumptions, the ADE reduces to a two-dimensional, second order partial differential equation as:

$$\frac{\partial C}{\partial t} = -u\frac{\partial C}{\partial x} + D_y\frac{\partial^2 C}{\partial y^2} \tag{2}$$

Analytical solutions to the above ADE exist for a variety of boundary and initial conditions (Van Genuchten et al., 2013). Assuming a semi-infinite longitudinal and finite-

transverse domain with a continuous line source (i.e. Farmland Input) at $x = 0$ and $y = 0$, the

steady-state solution for an infinite-width channel can be described as:

$$C = \frac{m}{2d\sqrt{\pi u D_y x}} \exp\left(-\frac{u y^2}{4 D_y x}\right) \tag{3}$$

where m is the rate of nitrate release into the river (kg N s^{-1}) and d is the flow depth (m). The

contaminant plume described above will eventually release the other bank of the river and a

mirror-image technique must be used to ensure that the constituent beyond the river bank is

reflected back (Van Genuchten et al., 2013). The concentration from equation (3) is amended as:

$$C^*(x,y) = C(x,y) + \sum_{n=1}^{\infty}[C(x, nB + (-1)^n y) + C(x, -nB + (-1)^n y)] \tag{4}$$

where B is the channel width (m) and n is the number of reflection cycles (usually set to 4 or 5).

The model was evaluated for average, steady-state conditions. Inputs to the ADE model

include data collected from the field and a lateral dispersion coefficient estimated from literature

(Table 1). The lateral dispersion coefficient (D_y) was estimated using an equation developed for

Missouri River (Huai et al., 2018) with similar frictional effects as:

$$D_y = 3.4 d u_* \tag{5}$$

where u_* is shear velocity ($u_* = \sqrt{gHS}$) (m s^{-1}) and S is the channel slope (m m^{-1}).

Table A1. Parameters for the advective-dispersion model of nitrate transport including parameter description, value, units, and references. "NA" signifies not applicable.

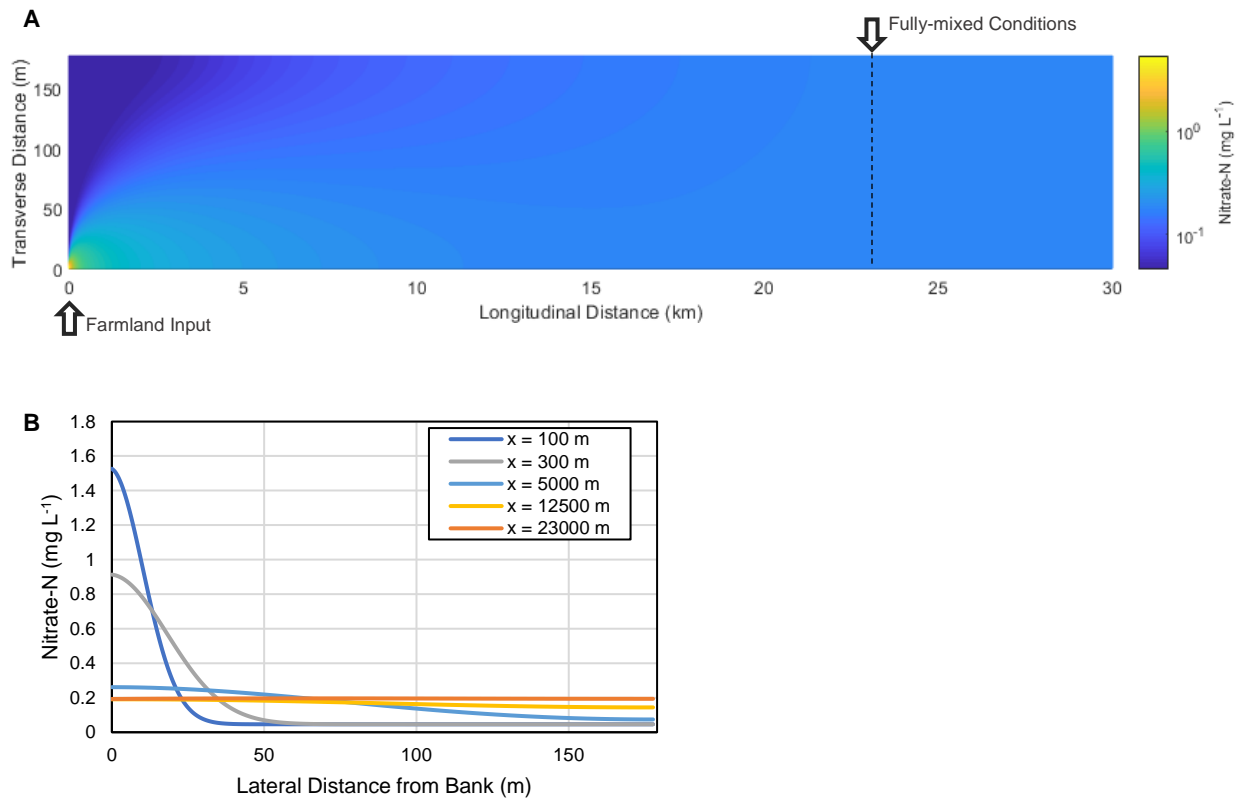| Parameter	Description	Value	Units	Reference(s)
S	Channel slope	0.042	%	(Simons, Li, & Associates, 1984)
d	Flow depth	0.97	m	
B	Channel width	179	m	
Q	Flow discharge	62	$m^3\ s^{-1}$	Measured on site
m	Farmland nitrate load	0.0071	$kg\ N\ s^{-1}$	
u_*	Shear velocity	0.06	$m\ s^{-1}$	(Huai et al., 2018)
D_y	Lateral dispersion coefficient	0.21	$m^2\ s^{-1}$	
n	Reflection cycles	4	NA	(Van Genuchten et al., 2013)

Figure A1. Results for the advective-dispersion model for the Kanas River. Fully-mixed conditions for mean loading and flow conditions occurs at $x = 23.54$ km (A). The lateral nitrate concentration profile at progressive downstream distance from the Farmland Input (B). Although fully-mixed conditions are realized at $x = 23.54$ km, the Kansas River is approximately fully-mixed at $x = 12.50$ km.